Colloid Polym Sci (2005) 283: 975–981
DOI 10.1007/s00396-004-1246-5

ORIGINAL CONTRIBUTIONS

Hidemi Iyota
Rumen Krastev
Hans-Joachim Müller

Thermodynamic studies on thin liquid films. III: Miscibility in adsorbed films at film interfaces

Received: 30 April 2004
Accepted: 8 October 2004

H. Iyota (✉)
Department of Life and Environmental Science, Kagoshima Prefectural College, 1-52-1, Shimoishiki, Kagoshima 890-0005, Japan
E-mail: iyota@k-kentan.ac.jp

R. Krastev · H.-J. Müller
Max-Planck-Institute of Colloids and Interfaces, D-14476 Golm, Germany

Abstract Thermodynamic treatment of surfactant mixture was developed for the adsorption at interfaces of thin liquid films and applied to the study of the foam film stabilized by decyl methyl sulfoxide (DeMS) in the presence of NaCl. The total surface density of NaCl and DeMS and the mole fraction of DeMS in the adsorbed film at the film surface were numerically evaluated by applying thermodynamic equations to the film tension as a function of the total molality of NaCl and DeMS and the mole fraction of DeMS in the mixture. Miscibility of NaCl and DeMS at the film surface was clarified by a phase diagram of adsorption and compared with that at the meniscus adjacent to the foam film. Judging from a phase diagram of phase transition, the transition in the DeMS foam film between common black and Newton black films, observed in part II, is a negative azeotropic transformation caused by the attractive interaction between the head group of DeMS molecule and Na^+ or Cl^- in the adsorbed film.

Keywords Miscibility in adsorbed film · Mixture of NaCl and decyl methyl sulfoxide · Common black and Newton black films · Phase transition in foam film · Negative azeotropy in phase transition · Thermodynamics of thin liquid films

Introduction

In part II of this series, the structure and properties of the foam-black film stabilized by decyl methyl sulfoxide (DeMS) were elucidated in terms of the surface densities of NaCl and DeMS at the film surfaces and the equivalent film thickness [1]. On the other hand, it has been shown for the mixed adsorption of surfactants at bulk interfaces that the evaluation of composition of an adsorbed film and drawing the phase diagram of adsorption is an useful strategy to clarify the miscibility of components and molecular interaction in the adsorbed film [2–9]. Furthermore, the thermodynamic treatment was applied not only to surfactant mixtures, but also to the mixtures of alkanol and surfactant [10–14], inorganic salt and surfactant [15–17], and proved to be highly useful to investigate the miscibility and molecular interaction in an oriented molecular state. This study aims to develop the thermodynamic treatment of surfactant mixture for the adsorption at film interfaces and apply the resultant equations to the film tension of a NaCl–DeMS mixture as a function of the total molality of the mixture and the mole fraction of DeMS in the mixture at 298.15 K under atmospheric pressure and constant disjoining pressure, shown in part II.

Theoretical

Fundamental equation for a thin liquid film formed from aqueous solutions of a binary electrolyte mixture having no common ions in which electrolyte 1 dissociates into $\nu_{1,a}$ a-ions and $\nu_{1,c}$ c-ions and electrolyte 2 into $\nu_{2,b}$ b-ions and $\nu_{2,d}$ d-ions is

$$\mathrm{d}\gamma^{\mathrm{f}} = -s^{\mathrm{f}}\mathrm{d}T + v^{\mathrm{f}}\mathrm{d}p + v^{\mathrm{L}}\mathrm{d}\Pi - \Gamma_a^{\mathrm{f}}\mathrm{d}\mu_a - \Gamma_c^{\mathrm{f}}\mathrm{d}\mu_c - \Gamma_b^{\mathrm{f}}\mathrm{d}\mu_b - \Gamma_d^{\mathrm{f}}\mathrm{d}\mu_d, \tag{1}$$

where γ^{f} is film tension, μ_j the chemical potential of j-ion, Γ_j^{f} the film density of j-ion, y^{f} the corresponding thermodynamic quantity, and v^{L} the volume of the phase L in the film per unit film area defined in part I [18] and II [1]. Taking the total molality $\hat{m}$ of the mixture and the mole fraction $\hat{X}_2$ of electrolyte 2 in the mixture as experimental variables in addition to temperature T, pressure p in the phase surrounding the film and disjoining pressure Π, and substituting the differentials of the chemical potentials

$$\mathrm{d}\mu_j = -s_j\mathrm{d}T + v_j\mathrm{d}p - v_j\mathrm{d}\Pi + \frac{RT}{\hat{m}}\mathrm{d}\hat{m} - \frac{RT}{\hat{X}_1}\mathrm{d}\hat{X}_2, \quad j = a, c, \tag{2}$$

and

$$\mathrm{d}\mu_j = -s_j\mathrm{d}T + v_j\mathrm{d}p - v_j\mathrm{d}\Pi + \frac{RT}{\hat{m}}\mathrm{d}\hat{m} + \frac{RT}{\hat{X}_2}\mathrm{d}\hat{X}_2, \quad j = b, d, \tag{3}$$

into Eq. 1, we obtain

$$\mathrm{d}\gamma^{f} = -\Delta s^{\mathrm{f}}\mathrm{d}T + \Delta v^{\mathrm{f}}\mathrm{d}p + \tau^{\mathrm{f}}\mathrm{d}\Pi - \frac{RT\hat{\Gamma}^{\mathrm{f}}}{\hat{m}}\mathrm{d}\hat{m} - \frac{RT\hat{\Gamma}^{\mathrm{f}}}{\hat{X}_1\hat{X}_2}(\hat{X}_2^{\mathrm{f}} - \hat{X}_2)\mathrm{d}\hat{X}_2, \tag{4}$$

assuming the film forming solution to be an ideal one. Here, $\hat{m}$ and $\hat{X}_2$ are defined by

$$\hat{m} = m_a + m_c + m_b + m_d = \nu_1 m_1 + \nu_2 m_2 \tag{5}$$

and

$$\hat{X}_2 = \frac{m_b + m_d}{\hat{m}} = \frac{\nu_2 m_2}{\hat{m}}, \tag{6}$$

m_i and m_j are the molalities of electrolyte i and j-ion, respectively and ν_1 and ν_2 denoting

$$\nu_1 = \nu_{1,a} + \nu_{1,c}, \quad \nu_2 = \nu_{2,b} + \nu_{2,d}. \tag{7}$$

The total film density $\hat{\Gamma}^{\mathrm{f}}$ of the mixture and the film mole fraction $\hat{X}_2^{\mathrm{f}}$ of electrolyte 2 in the mixture are defined by

$$\hat{\Gamma}^{\mathrm{f}} = \Gamma_a^{\mathrm{f}} + \Gamma_c^{\mathrm{f}} + \Gamma_b^{\mathrm{f}} + \Gamma_d^{\mathrm{f}} = \nu_1\Gamma_1^{\mathrm{f}} + \nu_2\Gamma_2^{\mathrm{f}} \tag{8}$$

and

$$\hat{X}_2^{\mathrm{f}} = \frac{\Gamma_b^{\mathrm{f}} + \Gamma_d^{\mathrm{f}}}{\hat{\Gamma}^{\mathrm{f}}} = \frac{\nu_2\Gamma_2^{\mathrm{f}}}{\hat{\Gamma}^{\mathrm{f}}}, \tag{9}$$

where the film density Γ_i^{f} of electrolyte i is given by Eq. 10 in part II. The thermodynamic quantity change Δy^{f} associated with adsorption at film interfaces and the thermodynamic film thickness τ^{f} are expressed by Eqs. 11 and 12 in part II.

Hence, $\Delta y^{\mathrm{f}}, \tau^{\mathrm{f}}, \hat{\Gamma}^{\mathrm{f}}$, and $\hat{X}_2^{\mathrm{f}}$ are related to γ^{f} by

$$\Delta s^{\mathrm{f}} = -\left(\frac{\partial\gamma^{\mathrm{f}}}{\partial T}\right)_{p,\Pi,\hat{m},\hat{X}_2}, \tag{10}$$

$$\Delta v^{\mathrm{f}} = \left(\frac{\partial\gamma^{\mathrm{f}}}{\partial p}\right)_{T,\Pi,\hat{m},\hat{X}_2}, \tag{11}$$

$$\tau^{\mathrm{f}} = \left(\frac{\partial\gamma^{\mathrm{f}}}{\partial \Pi}\right)_{T,p,\hat{m},\hat{X}_2}, \tag{12}$$

$$\hat{\Gamma}^{\mathrm{f}} = -\left(\frac{\hat{m}}{RT}\right)\left(\frac{\partial\gamma^{\mathrm{f}}}{\partial \hat{m}}\right)_{T,p,\Pi,\hat{X}_2}, \tag{13}$$

and

$$\hat{X}_2^{\mathrm{f}} = \hat{X}_2 - \left(\frac{\hat{X}_1\hat{X}_2}{RT\hat{\Gamma}^{\mathrm{f}}}\right)\left(\frac{\partial\gamma^{\mathrm{f}}}{\partial \hat{X}_2}\right)_{T,p,\Pi,\hat{m}} \tag{14}$$

$$\hat{X}_2^{\mathrm{f}} = \hat{X}_2 - \left(\frac{\hat{X}_1\hat{X}_2}{\hat{m}}\right)\left(\frac{\partial\hat{m}}{\partial \hat{X}_2}\right)_{T,p,\Pi,\gamma^{\mathrm{f}}}, \tag{15}$$

The corresponding energy and enthalpy changes are given by the same equations as Eqs. 47 and 48 in part I, respectively.

On the other hand, Eq. 49 in part I, for the interfacial tension of the meniscus adjacent to the film, can be rewritten for the present mixture in the form

$$\mathrm{d}\gamma_{\mathrm{K}} = -\Delta s_{\mathrm{K}}\mathrm{d}T + \Delta v_{\mathrm{K}}\mathrm{d}p + (v_{\mathrm{K}}^{\mathrm{H,K}} - \Delta v_{\mathrm{K}})\mathrm{d}\Pi - \left(\frac{RT\hat{\Gamma}^{\mathrm{H,K}}}{\hat{m}}\right)\mathrm{d}\hat{m} - \left(\frac{RT\hat{\Gamma}^{\mathrm{H,K}}}{\hat{X}_1\hat{X}_2}\right)(\hat{X}_2^{\mathrm{H,K}} - \hat{X}_2)\mathrm{d}\hat{X}_2, \quad \mathrm{K} = \mathrm{A}, \mathrm{B}. \tag{16}$$

Hence, the combination of Eq. 4 with Eq. 16 yields the differences in the thermodynamic quantities between the film and the adjacent meniscuses

$$\Delta s^{\mathrm{f}} - \Delta s_{\mathrm{A}} - \Delta s_{\mathrm{B}} = -\left[\frac{\partial(\gamma^{\mathrm{f}} - \gamma_{\mathrm{A}} - \gamma_{\mathrm{B}})}{\partial T}\right]_{p,\Pi,\hat{m},\hat{X}_2}, \tag{17}$$

$$\Delta v^{\mathrm{f}} - \Delta v_{\mathrm{A}} - \Delta v_{\mathrm{B}} = -\left[\frac{\partial(\gamma^{\mathrm{f}} - \gamma_{\mathrm{A}} - \gamma_{\mathrm{B}})}{\partial p}\right]_{p,\Pi,\hat{m},\hat{X}_2}, \tag{18}$$

$$\tau^{\mathrm{f}} - v_{\mathrm{A}}^{\mathrm{H,A}} - v_{\mathrm{B}}^{\mathrm{H,B}} + \Delta v_{\mathrm{A}} + \Delta v_{\mathrm{B}} = \left[\frac{\partial(\gamma^{\mathrm{f}} - \gamma_{\mathrm{A}} - \gamma_{\mathrm{B}})}{\partial \Pi}\right]_{T,p,\hat{m},\hat{X}_2}, \tag{19}$$

$$\hat{\Gamma}^{\mathrm{f}} - \hat{\Gamma}^{\mathrm{H,A}} - \hat{\Gamma}^{\mathrm{H,B}} = -\left(\frac{\hat{m}}{RT}\right)\times \left[\frac{\partial(\gamma^{\mathrm{f}} - \gamma_{\mathrm{A}} - \gamma_{\mathrm{B}})}{\partial \hat{m}}\right]_{T,p,\Pi,\hat{X}_2}, \tag{20}$$

and

$$\hat{\Gamma}^{\mathrm{f}}(\hat{X}_2^{\mathrm{f}} - \hat{X}_2) - \hat{\Gamma}^{\mathrm{H,A}}(\hat{X}_2^{\mathrm{H,A}} - \hat{X}_2) - \hat{\Gamma}^{\mathrm{H,B}}(\hat{X}_2^{\mathrm{H,B}} - \hat{X}_2) = -\left(\frac{\hat{X}_1\hat{X}_2}{RT}\right)\left[\frac{\partial(\gamma^{\mathrm{f}} - \gamma_{\mathrm{A}} - \gamma_{\mathrm{B}})}{\partial \hat{X}_2}\right]_{T,p,\Pi,\hat{m}}, \tag{21}$$

The corresponding equations for the differences in energy and enthalpy are the same as Eqs. 62 and 63 in part I, respectively.

For a symmetric film, let $\hat{\Gamma}^{\mathrm{F}}$, $\hat{X}_2^{\mathrm{F}}$, Δy^{F}, and γ be the total interfacial density at a film interface, the mole fraction of component 2 in the adsorbed film at the film interface, the thermodynamic quantity change associated with adsorption at the film interface, and the interfacial tension of the meniscus adjacent to the film, respectively. We have then

$$\frac{1}{2}\hat{\Gamma}^{\mathrm{f}} = \hat{\Gamma}^{\mathrm{F}} = \Gamma_a^{\mathrm{F}} + \Gamma_c^{\mathrm{F}} + \Gamma_b^{\mathrm{F}} + \Gamma_d^{\mathrm{F}} = v_1\Gamma_1^{\mathrm{F}} + v_2\Gamma_2^{\mathrm{F}}, \tag{22}$$

$$\hat{X}_2^{\mathrm{f}} = \hat{X}_2^{\mathrm{F}} = \frac{\Gamma_b^{\mathrm{F}} + \Gamma_d^{\mathrm{F}}}{\hat{\Gamma}^{\mathrm{F}}} = \frac{v_2\Gamma_2^{\mathrm{F}}}{\hat{\Gamma}^{\mathrm{F}}}, \tag{23}$$

and

$$\frac{1}{2}\Delta y^{\mathrm{f}} = \Delta y^{\mathrm{F}}, \tag{24}$$

where the interfacial densities Γ_i^{F} of electrolyte i and Γ_j^{F} of j-ion at the film interface and Δy^{F} are defined in a manner similar to Eq. 10 in part II and Eqs. 16 and 59 in part I, respectively. Substituting Eqs. 22, 23, and 24 into Eqs. 10 and 11 and Eqs. 13, 14, and 15 yields

$$\Delta s^{\mathrm{F}} = -\frac{1}{2}\left(\frac{\partial \gamma^{\mathrm{f}}}{\partial T}\right)_{p,\Pi,\hat{m},\hat{X}_2}, \tag{25}$$

$$\Delta v^{\mathrm{F}} = \frac{1}{2}\left(\frac{\partial \gamma^{\mathrm{f}}}{\partial p}\right)_{T,\Pi,\hat{m},\hat{X}_2}, \tag{26}$$

$$\hat{\Gamma}^{\mathrm{F}} = -\frac{1}{2}\left(\frac{\hat{m}}{RT}\right)\left(\frac{\partial \gamma^{\mathrm{f}}}{\partial \hat{m}}\right)_{T,p,\Pi,\hat{X}_2}, \tag{27}$$

and

$$\hat{X}_2^{\mathrm{F}} = \hat{X}_2 - \frac{1}{2}\left(\frac{\hat{X}_1\hat{X}_2}{RT\hat{\Gamma}^{\mathrm{F}}}\right)\left(\frac{\partial \gamma^{\mathrm{f}}}{\partial \hat{m}}\right)_{T,p,\Pi,\hat{X}_2}, \tag{28}$$

$$\hat{X}_2^{\mathrm{F}} = \hat{X}_2 - \left(\frac{\hat{X}_1\hat{X}_2}{\hat{m}}\right)\left(\frac{\partial \hat{m}}{\partial \hat{X}_2}\right)_{T,p,\Pi,\gamma^{\mathrm{f}}}. \tag{29}$$

Energy and enthalpy changes are given by

$$\Delta u^{\mathrm{F}} = T\Delta s^{\mathrm{F}} - p\Delta v^{\mathrm{F}} - \frac{1}{2}\Pi\tau^{\mathrm{f}} + \frac{1}{2}\gamma^{\mathrm{f}} \tag{30}$$

$$\Delta h^{\mathrm{F}} = T\Delta s^{\mathrm{F}}. \tag{31}$$

Equations 17, 18, 19, 20, and 21, similarly reduce to

$$\Delta s^{\mathrm{F}} - \Delta s = -\frac{1}{2}\left[\frac{\partial(\gamma^{\mathrm{f}} - 2\gamma)}{\partial T}\right]_{p,\Pi,\hat{m},\hat{X}_2} \tag{32}$$

$$\Delta v^{\mathrm{F}} - \Delta v = \frac{1}{2}\left[\frac{\partial(\gamma^{\mathrm{f}} - 2\gamma)}{\partial p}\right]_{T,\Pi,\hat{m},\hat{X}_2} \tag{33}$$

$$\frac{1}{2}\tau^{\mathrm{f}} - v^{\mathrm{H,A}} + \Delta v = \frac{1}{2}\left[\frac{\partial(\gamma^{\mathrm{f}} - 2\gamma)}{\partial \Pi}\right]_{T,p,\hat{m},\hat{X}_2} \tag{34}$$

$$\hat{\Gamma}^{\mathrm{F}} - \hat{\Gamma}^{\mathrm{H}} = -\left(\frac{\hat{m}}{2RT}\right)\left[\frac{\partial(\gamma^{\mathrm{f}} - 2\gamma)}{\partial \hat{m}}\right]_{T,p,\Pi,\hat{X}_2}, \tag{35}$$

and

$$\hat{\Gamma}^{\mathrm{F}}(\hat{X}_2^{\mathrm{F}} - \hat{X}_2) - \hat{\Gamma}^{\mathrm{H}}(\hat{X}_2^{\mathrm{H}} - \hat{X}_2) = -\left(\frac{\hat{X}_1\hat{X}_2}{2RT}\right)\left[\frac{\partial(\gamma^{\mathrm{f}} - 2\gamma)}{\partial \hat{X}_2}\right]_{T,p,\Pi,\hat{m}}. \tag{36}$$

Energy and enthalpy changes are given by the same expressions as Eqs. 80 and 81 in part I.

Results and discussion

Let us apply the above thermodynamic treatment to the foam film formed from the NaCl–DeMS mixture in part II of this series. For the mixture of uni–univalent electrolyte 1 and nonionic surfactant 2, we have

$$v_{1,a} = v_{1,c} = 1, \quad v_{2,b} = 1 \text{ and } v_{2,d} = 0, \tag{37}$$

and Eqs. 5, 6, 22, and 23 reduce to

$$\hat{m} = 2m_1 + m_2, \tag{38}$$

$$\hat{X}_2 = \frac{m_2}{\hat{m}}, \tag{39}$$

$$\hat{\Gamma}^{\mathrm{F}} = 2\Gamma_1^{\mathrm{F}} + \Gamma_2^{\mathrm{F}}, \tag{40}$$

and

$$\hat{X}_2^{\mathrm{F}} = \frac{\Gamma_2^{\mathrm{F}}}{\hat{\Gamma}^{\mathrm{F}}}, \tag{41}$$

respectively.

Numerical values of the difference between γ^{f} and 2γ of the NaCl–DeMS system were obtained by substituting the values of contact angle θ in Fig. 2 in part II and the surface tension γ of film-forming solutions in the previous study [19] into the equation

$$\gamma^{\mathrm{f}} - 2\gamma = 2\gamma(\cos\theta - 1), \tag{42}$$

assuming that the $\tau\Pi$ term in Eq. 64 in part I is negligible. $\gamma^{\mathrm{f}}-2\gamma$ is shown as a function of $\hat{m}$ in Fig. 1, in which typical errors arising from the error in θ are shown for curve 3. For the equilibrium film with positive Π formed in a ring cell, γ^{f} is less than 2γ, γ^{f} of a thick film, due to the interaction between film interfaces. An arrow on the $\gamma^{\mathrm{f}}-2\gamma$ versus $\hat{m}$ curve designates the phase transition in the black film determined from the jump in the equilibrium film thickness and the break on the contact angle versus total molality curve in Figs. 1 and 2 in part II. We see that $\gamma^{\mathrm{f}}-2\gamma$ decreases with increase in $\hat{m}$ and decreases more greatly after the phase transition. It is worth noting that $\gamma^{\mathrm{f}}-2\gamma$ versus $\hat{m}$ curve of the lowest $\hat{X}_2$ has a minimum unlike those of the other $\hat{X}_2'$s. Figure 2 presents the $\hat{m}$ value at a given γ^{f}, taken from the γ^{f} versus $\hat{m}$ curve obtained from the $\gamma^{\mathrm{f}}-2\gamma$ in Fig. 1 and γ, as a function of $\hat{X}_2$. It is seen that there is a steep rise in $\hat{m}$ with decreasing $\hat{X}_2$ at very low $\hat{X}_2$. The values of the film tension $\gamma^{\mathrm{f,eq}}$ and total molality $\hat{m}^{\mathrm{eq}}$ at the phase transition where common black and Newton black films coexist at equilibrium, read from the γ^{f} versus $\hat{m}$ curve and Figs. 1 and 2 in part II, are plotted against $\hat{X}_2$ in Fig. 3a and b, respectively. The values of the surface tension γ^{c} at the CMC and CMC, $\hat{C}$ of the mixture obtained in the previous study [19], are also shown in the forms of the $2\gamma^{\mathrm{c}}$ versus $\hat{X}_2$ and $\hat{C}$ versus $\hat{X}_2$ curves in the figures, respectively; the $\gamma^{\mathrm{f,eq}}$ versus $\hat{X}_2$ and $2\gamma^{\mathrm{c}}$ versus $\hat{X}_2$ curves coincide with each other at $\hat{X}_2 = 0.014$ and 0.8, as well as the $\hat{m}^{\mathrm{eq}}$ versus $\hat{X}_2$ and $\hat{C}$ versus $\hat{X}_2$ curves; $\gamma^{\mathrm{f,eq}}$ is larger than $2\gamma^{\mathrm{c}}$ and $\hat{m}^{\mathrm{eq}}$ is smaller than $\hat{C}$ at $\hat{X}_2$ between 0.014 and 0.8. Equations derived in the last section can be applied to the γ^{f} in the region of $\hat{m}$ below $\hat{C}$.

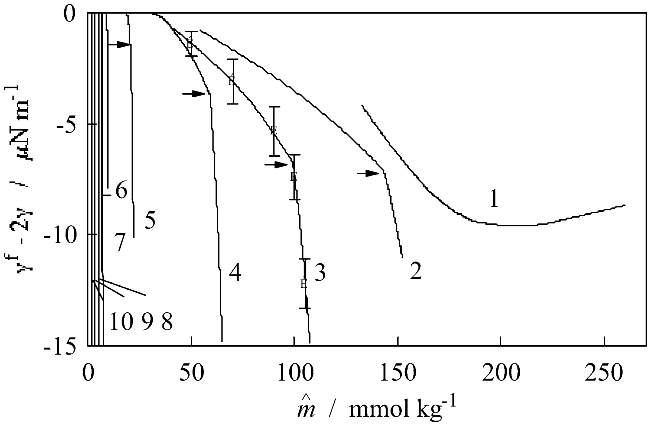

Fig. 1 Difference between film tension and surface tension versus total molality curves at a constant composition: (1) $\hat{X}_2$ =0.00772, (2) 0.01379, (3) 0.01810, (4) 0.03015, (5) 0.09173, (6) 0.2150, (7) 0.2884, (8) 0.3817, (9) 0.4984, and (10) 0.7999

Numerical value of $\hat{\Gamma}^{\mathrm{F}}$ evaluated by applying Eq. 27 to the γ^{f} versus $\hat{m}$ curve is shown as a function of $\hat{m}$ in Fig. 4a, together with the $\hat{\Gamma}^{\mathrm{H}}$ in the previous study [19]. The $\hat{\Gamma}^{\mathrm{F}}$ value of the common black film seems to be very similar to the $\hat{\Gamma}^{\mathrm{H}}$ value of the bulk surface coexisting in equilibrium with the black film and slightly jumps to that of the Newton black film at the transition. The $\hat{\Gamma}^{\mathrm{F}} - \hat{\Gamma}^{\mathrm{H}}$ value obtained by fitting Eq. 35 to the $\gamma^{\mathrm{f}}-2\gamma$ versus $\hat{m}$ curve in Fig. 1 is presented against $\hat{m}$ in Fig. 4b. We see $\hat{\Gamma}^{\mathrm{F}}$ is larger than $\hat{\Gamma}^{\mathrm{H}}$ and their difference increases as $\hat{m}$ increases. The decrease in $\hat{\Gamma}^{\mathrm{F}} - \hat{\Gamma}^{\mathrm{H}}$ with increasing $\hat{m}$ at the lowest $\hat{X}_2$ is due to the decreases both in $\Gamma_1{}^{\mathrm{F}}-\Gamma_1{}^{\mathrm{H}}$ of NaCl and $\Gamma_2{}^{\mathrm{F}}-\Gamma_2{}^{\mathrm{H}}$ of DeMS with increasing molality of NaCl as shown in part II. It is worth noting that the $\hat{\Gamma}^{\mathrm{F}} - \hat{\Gamma}^{\mathrm{H}}$ value is less than 0.5 % of the $\hat{\Gamma}^{\mathrm{H}}$ value, which is, however, characteristic of the formation of the black films and the cause of the transition in the film as shown by the calculation of the interaction force between film surfaces in part II.

To elucidate the miscibility of NaCl and DeMS in the adsorbed film at the film surface, $\hat{X}_2^{\mathrm{f}}$ was numerically evaluated by applying Eq. 29 to the $\hat{m}$ versus $\hat{X}_2$ curve in Fig. 2. The $\hat{X}_2^{\mathrm{f}}$ value is shown in the form of the $\hat{m}$ versus $\hat{X}_2^{\mathrm{f}}$ curve together with the $\hat{m}$ versus $\hat{X}_2$ in Fig. 5, which we call the phase diagram of adsorption at film surface because it exhibits the composition of the solution and the adsorbed film at film surface coexisting in equilibrium. $\hat{X}_2^{\mathrm{f}}$ smaller than unity in the diagram indicates that

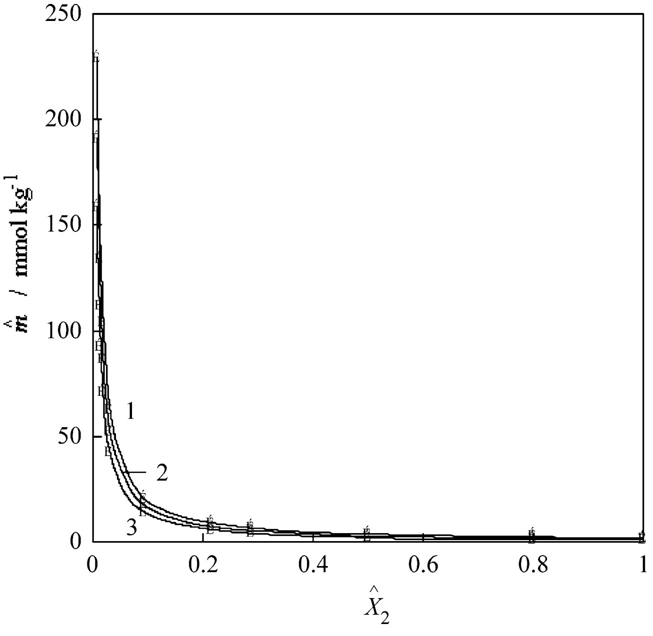

Fig. 2 Total molality versus composition curves at constant film tension: (1) γ^{f} = 50 mN m^{-1}, (2) 55, (3) 60

DeMS molecule is miscible with Na$^+$ or Cl$^-$ ions and the polar head group of DeMS molecule attracts Na$^+$ or Cl$^-$ in the adsorbed film at the film surface. An arrow on the $\hat{m}$ versus $\hat{X}_2^{\mathrm{f}}$ curve at 50 mN m^{-1} shows the transition in the black films. The difference in composition of an adsorbed film between the film and bulk surfaces are shown in the form of the $\hat{m}$ versus $\hat{X}_2^{\mathrm{F}} - \hat{X}_2^{\mathrm{H}}$ curve in Fig. 6a–c, where $\hat{X}_2^{\mathrm{F}} - \hat{X}_2^{\mathrm{H}}$ is numerically evaluated by applying Eq. 36 to the γ^{f}–2γ versus $\hat{X}_2$ curve obtained from Fig. 1 and substituting the $\hat{\Gamma}^{\mathrm{F}}$ and $\hat{\Gamma}^{\mathrm{H}}$ values into Eq. 36. $\hat{X}_2^{\mathrm{H}}$ in the previous study [19] was also used. Figure 6a indicates that $\hat{X}_2^{\mathrm{f}}$ is smaller than $\hat{X}_2^{\mathrm{H}}$ at higher γ^{f}, hence, NaCl and DeMS are miscible more in the adsorbed film of the common black film than in that of the bulk surface. It is noticed from Fig. 6b and c that two phase transitions take place as $\hat{m}$ increases at a given γ^{f}; both the transitions are accompanied by the increase in the miscibility of NaCl and DeMS. The increase in the miscibility on phase transition is attributable more to the increase in $\Gamma_1{}^{\mathrm{F}}$ at the transition point than to the corresponding change in $\Gamma_2{}^{\mathrm{F}}$ in part II, taking into consideration that γ^{f} is almost constant at constant m_2 for the NaCl–DeMS system. Electrical shielding of the surface charge due to the preferential adsorption of OH$^-$ ions [20, 21], at the surface of the Newton black film by the positive adsorption of NaCl is probably different between the Newton black films at the first transition at low $\hat{m}$ and at the second one at high $\hat{m}$.

The values of $\hat{X}_2^{\mathrm{F,c}}$ of the common black film and $\hat{X}_2^{\mathrm{F,N}}$ of the Newton black one at the phase transition, obtained from the $\hat{X}_2^{\mathrm{F}} - \hat{X}_2^{\mathrm{H}}$ at the transition in Fig. 6 and the $\hat{X}_2^{\mathrm{H}}$ in the previous study [19], were designated in the form of the $\gamma^{\mathrm{f,eq}}$ versus $\hat{X}_2^{\mathrm{F,c}}$ and $\gamma^{\mathrm{f,eq}}$ versus $\hat{X}_2^{\mathrm{F,N}}$

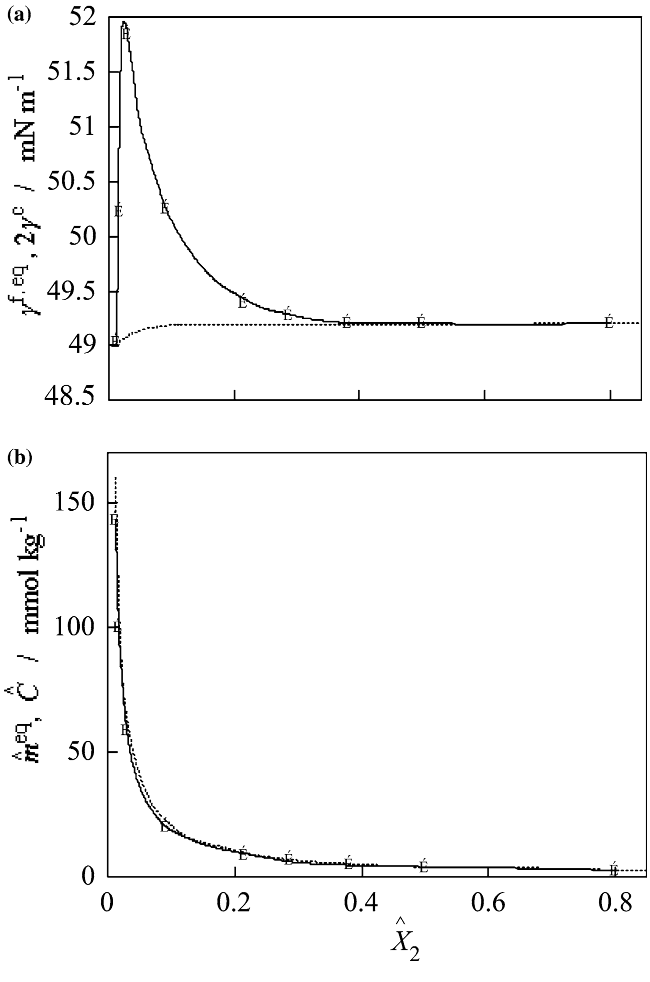

Fig. 3 (a) Film tension at phase transition versus and surface tension at CMC versus composition curves; (*solid lines*) $\gamma^{\mathrm{f,eq}}$ versus $\hat{X}_2$, (*dotted lines*) $2\gamma^{\mathrm{c}}$ versus $\hat{X}_2$; (b) total molality at phase transition versus and CMC versus composition curves; (*solid lines*) $\hat{m}^{\mathrm{eq}}$ versus $\hat{X}_2$, (*dotted lines*) $\hat{C}$ versus $\hat{X}_2$

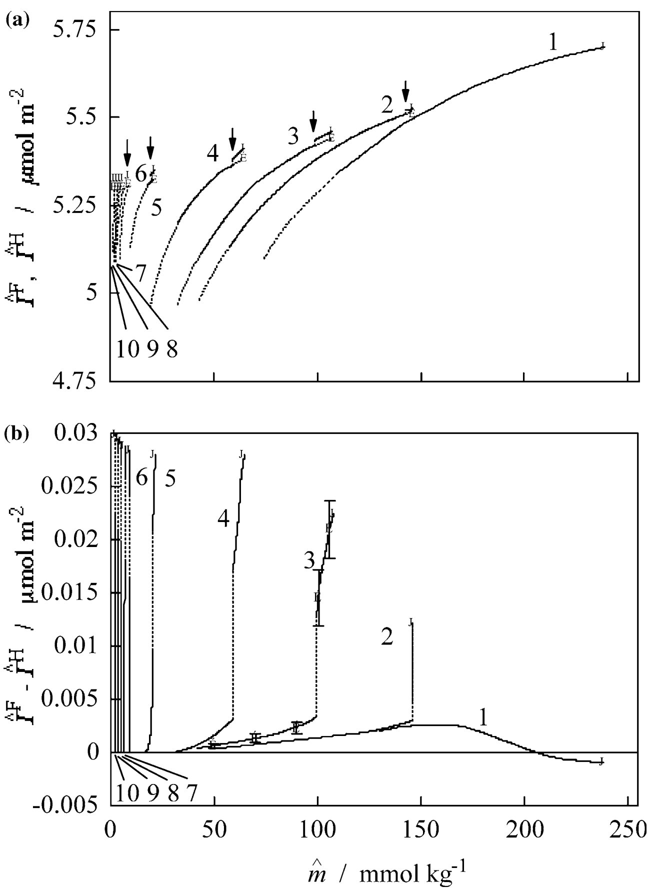

Fig. 4 (**a**) Total surface density versus total molality curves at constant composition; (*solid lines*) $\hat{\Gamma}^{\mathrm{F}}$ versus $\hat{m}$, (*dotted lines*) $\hat{\Gamma}^{\mathrm{H}}$ versus $\hat{m}$; and (J) $\hat{\Gamma}^{\mathrm{F}}$ at the CMC, (E) $\hat{\Gamma}^{\mathrm{H}}$ at the CMC; (**b**) difference in total surface density versus total molality curves at constant composition; (J) $\hat{\Gamma}^{\mathrm{F}} - \hat{\Gamma}^{\mathrm{H}}$ at the CMC: (1) $\hat{X}_2$ =0.00772, (2) 0.01379, (3) 0.01810, (4) 0.03015, (5) 0.09173, (6) 0.2150, (7) 0.2884, (8) 0.3817, (9) 0.4984, and (10) 0.7999

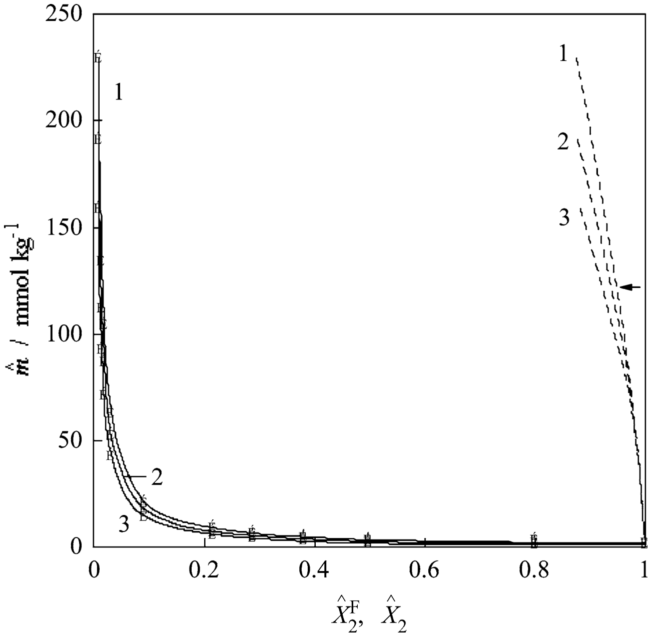

Fig. 5 Total molality versus composition curves at constant film tension: (1) $\gamma^f = 50$ mN m^{-1}, (2) 55, (3) 60; (*dotted lines*) $\hat{m}$ versus $\hat{X}_2^F$, (*solid lines*) $\hat{m}$ versus $\hat{X}_2$

curves in Fig. 7. We call Fig. 7 the phase diagram of phase transition. The two curves in the diagram have the maximum at which they coincide, which is typical of negative azeotropic mixtures [22]. Therefore, we conclude that negative azeotropic transformation takes place in the black film caused by the attractive interaction between the head group of the DeMS molecule and Na$^+$ or Cl$^-$ in the adsorbed film at the film surface and the interaction is larger in the Newton black film than in the common black film.

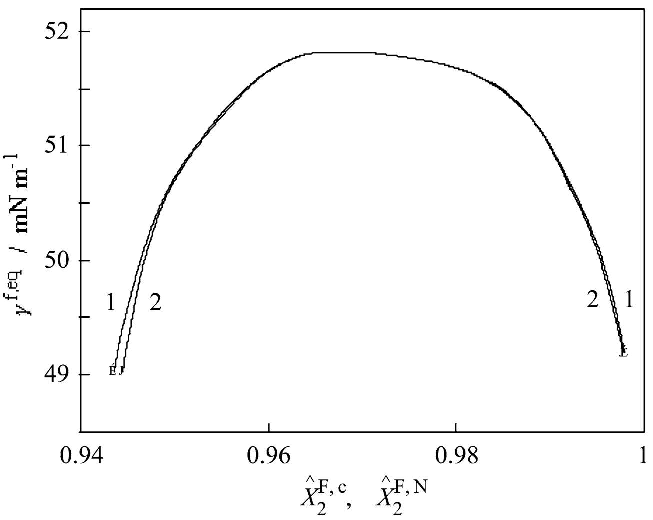

Fig. 7 Film tension at phase transition versus composition curves: (1) $\hat{X}_2^{F,c}$, (2) $\hat{X}_2^{F,N}$; and (*open circle*) $\hat{X}_2^{F,c}$ at the CMC, and (*solid circle*) $\hat{X}_2^{F,N}$ at the CMC

At the phase transition, Eq. 4 reduces to

$$d\gamma^{f,eq} = -2\Delta s^{F,c}dT + 2\Delta v^{F,c}dp + \tau^{f,c}d\Pi - 2\left(\frac{RT\hat{\Gamma}^{F,c}}{\hat{m}}\right)d\hat{m} - 2\left(\frac{RT\hat{\Gamma}^{F,c}}{\hat{X}_1\hat{X}_2}\right)(\hat{X}_2^{F,c} - \hat{X}_2)d\hat{X}_2 \tag{43}$$

$$d\gamma^{f,eq} = -2\Delta s^{F,N}dT + 2\Delta v^{F,N}dp + \tau^{f,N}d\Pi - 2\left(\frac{RT\hat{\Gamma}^{F,N}}{\hat{m}}\right)d\hat{m} - 2\left(\frac{RT\hat{\Gamma}^{F,N}}{\hat{X}_1\hat{X}_2}\right)(\hat{X}_2^{F,N} - \hat{X}_2)d\hat{X}_2 \tag{44}$$

Fig. 6 Total molality versus composition difference curves at constant film tension: (**a**) (1) $\gamma^f = 60$ mN m^{-1}, (2) 55; (**b**) 51.3; and (**c**) 50

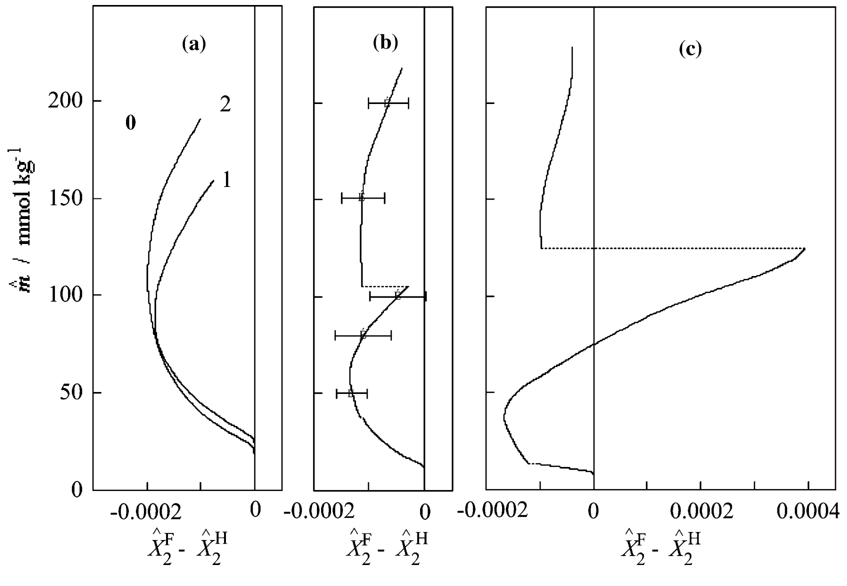

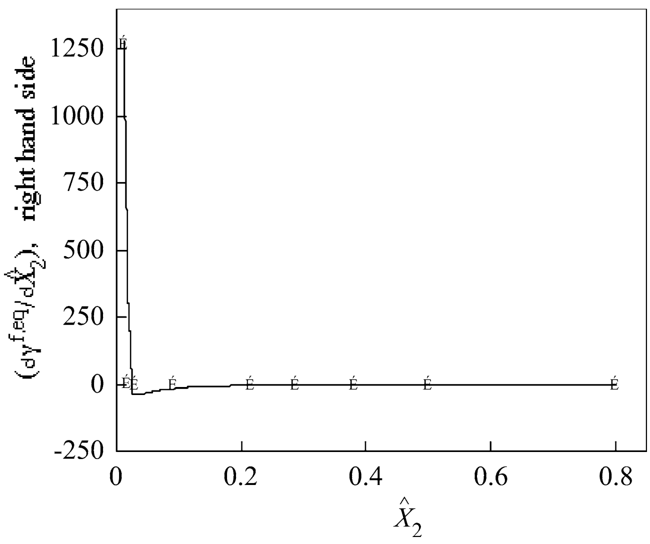

Fig. 8 Left- and right-hand sides of Eq. 45 versus composition curve: (*solid lines*) left-hand side, (*open circle*) right-hand side

for the common black and Newton black films of which the thermodynamic quantities are denoted by superscripts c and N, respectively. Eliminating the term $\mathrm{d}\hat{m}$ from Eqs. 43 and 44 at constant T, p, and Π leads to

$$\left(\frac{\partial \gamma^{\mathrm{f,eq}}}{\partial X_2}\right)_{T,p,\Pi} = -\frac{(2RT/\hat{X}_1\hat{X}_2)(\hat{X}_2^{\mathrm{F,N}} - \hat{X}_2^{\mathrm{F,c}})}{(\hat{\Gamma}^{\mathrm{F,N}})^{-1} - (\hat{\Gamma}^{\mathrm{F,c}})^{-1}}. \qquad (45)$$

Numerical values of both sides of Eq. 45 can be independently obtained: the left-hand side is obtained from the $\gamma^{\mathrm{f,eq}}$ versus $\hat{X}_2$ curve in Fig. 3a, on the other hand, the right-hand side is calculated by use of the $\hat{\Gamma}^{\mathrm{F}}$ and $\hat{X}_2^{\mathrm{f}}$ values at the transition shown in Figs. 4a and 5, respectively. The values of both sides shown as a function of $\hat{X}_2$ in Fig. 8 are in good agreement. Therefore, the phase transition between the common black and the Newton black films is a first order one. The above conclusion is in conformity with the jump in equivalent film thickness and the break on the contact angle versus total molality curve at the transition point shown in Figs. 1 and 2 in part II, because the film thickness is related to the first derivative of film tension as in Eq. 12.

Conclusions

From the present study, the following conclusions can be drawn.

1. Miscibility and interaction in the adsorbed films at film interfaces can be clarified by applying the thermodynamic equations for a surfactant mixture to the film tension as a function of the total molality and the mole fraction in the mixture at constant temperature, pressure, and disjoining pressure.
2. Miscibility of NaCl and DeMS in the adsorbed film of the common black film is larger than that at the bulk surface adjacent to and in equilibrium with the black film.
3. The phase transition in the DeMS foam film between the common black and Newton black films is a first-order and negative azeotropic transformation caused by the attractive interaction between the head group of the DeMS molecule and Na^{+} or Cl^{-} in the adsorbed film at the film surface.
4. The attractive interaction is larger in the Newton black film than in the common black film.

References

1. Iyota H, Krustev R, Müller H-J (2004) Colloid Polym Sci 282(12):1392–1402
2. Motomura K, Ando N, Matsuki H, Aratono M (1990) J Colloid Interface Sci 139:188
3. Matsuki H, Ikeda N, Aratono M, Kaneshina S, Motomura K (1992) J Colloid Interface Sci 154:454
4. Motomura K, Kanda T, Abe K, Todoroki N, Ikeda N, Aratono M (1992) Colloids Surf 67:53
5. Todoroki N, Tanaka F, Ikeda N, Aratono M, Motomura K (1993) Bull Chem Soc Jpn 66:351
6. Motomura K, Aratono M (1993) Miscibility in binary mixtures of surfactants In: Ogino K, Abe M (eds) Mixed surfactant systems. Surfactant Sci Ser 46. Marcel Dekker, New York, pp 99–144
7. Takiue T, Tomioka M, Ikeda M, Matsubara A, Aratono M, Motomura K (1996) Colloid Polym Sci 274:470
8. Aratono M, Ikeguchi M, Takiue T, Ikeda N, Motomura K (1995) J Colloid Interface Sci 174:156
9. Iyota H, Todoroki N, Ikeda N, Motomura K, Ohta A, Aratono M (1999) J Colloid Interface Sci 216:41
10. Matsuki H, Kanda T, Aratono M, Motomura K (1993) Bull Chem Soc Jpn 63:2159
11. Iyota H, Motomura K (1992) J Colloid Interface Sci 148:369
12. Iyota H, Tomimitsu T, Motomura K, Aratono M (1998) Langmuir 14:5347
13. Ikeda N, Tsukamoto A, Murakado C, Villeneuve M, Takiue T, Aratono M, Motomura K (1998) Colloid Polym Sci 276:267
14. Villeneuve M, Ikeda N, Motomura K, Aratone M (1998) J Colloid Interface Sci 208:388
15. Yamanaka M, Matsuki H, Ikeda N, Aratono M, Motomura K (1994) Langmuir 10:2950
16. Matsubara H, Ohta A, Kameda M, Villeneuve M, Ikeda N, Aratono M, (1999) Langmuir 15:5496
17. Iyota H, Shimada K, Abe K, Ikeda N, Motomura K, Aratono M (2001) J Colloid Interface Sci 234:322
18. Iyota H, Kvustev R, Müller H-J (2004) Colloid Polym Sci 282:1329
19. Iyota H, Tomimitsu T (2003) J Colloid Interface Sci 257:327
20. Exerowa D, Zacharieva M, Cohen R, Platikanov D (1979) Colloid Polym Sci 257:1089
21. Manev ED, Pugh RJ (1991) Langmuir 7:2253
22. Rawlinson JS, Swinton FL (1982) Liquids and liquid mixtures, chap 4, 3rd edn. Butterworth, London